environmental microbiology

Environmental Microbiology (2010) **12**(7), 1899–1912 doi:10.1111/j.1462-2920.2010.02195.x

Regulation of nitrogen metabolism in the marine diazotroph *Trichodesmium* IMS101 under varying temperatures and atmospheric CO_2 concentrations

Orly Levitan,[1] Christopher M. Brown,[2†] Stefanie Sudhaus,[3] Douglas Campbell,[2] Julie LaRoche[3] and Ilana Berman-Frank[1*]

[1]*The Mina and Everard Goodman Faculty of Life Sciences, Bar Ilan University, Ramat Gan, 52900, Israel.*
[2]*Department of Biology, Mount Allison University, Sackville, NB E4L 1G7, Canada.*
[3]*IFM-GEOMAR, Leibniz Institute of Marine Sciences at Kiel University, 24105 Kiel, Germany.*

Summary

We examined the influence of forecasted changes in global temperatures and pCO_2 on N_2 fixation and assimilation in the ecologically important cyanobacterium *Trichodesmium* spp. Changes of mRNA transcripts (*nifH, glnA, hetR, psbA, psaB*), protein (nitrogenase, glutamine synthetase) pools and enzymatic activity (nitrogenase) were measured under varying pCO_2 and temperatures. High pCO_2 shifted transcript patterns of all genes, resulting in a more synchronized diel expression. Under the same conditions, we did not observe any significant changes in the protein pools or in total cellular allocations of carbon and nitrogen (i.e. C : N ratio remained stable). Independently of temperature, high pCO_2 (900 μatm) elevated N_2 fixation rates. Levels of the key enzymes, nitrogenase and glutamine synthetase that mediate nitrogen assimilation did not increase, implying that the high pCO_2 allowed higher reaction turnover rates through these key enzymes. Moreover, increased temperatures and high pCO_2 resulted in higher C : P ratios. The plasticity in phosphorous stoichiometry combined with higher enzymatic efficiencies lead to higher growth rates. In cyanobacteria photosynthesis, carbon uptake, respiration, N_2 fixation and nitrogen assimilation share cellular components. We propose that shifted cellular resource and energy allocation among those components will enable *Trichodesmium* grown at elevated temperatures and pCO_2 to extend its niche in the future ocean, through both tolerance of a broader temperature range and higher P plasticity.

Received 29 June, 2009; accepted 22 January, 2010. *For correspondence. E-mail irfrank@mail.biu.ac.il; Tel. (+972) 3 5318214; Fax (+972) 3 5318214. †Present address: Institute of Marine and Coastal Sciences, School of Environmental and Biological Sciences, Rutgers University, New Brunswick, NJ 08901, USA.

Introduction

Key phytoplankton species contributing to oceanic primary production and global biogeochemical nutrient cycles may be significantly affected by oceanic acidification and the global increases in temperatures and atmospheric pCO_2. One such species is the marine nitrogen-fixing (diazotroph) cyanobacterium *Trichodesmium* spp. contributing 25–50% of the geochemically derived rates of N_2 fixation in various ocean basins, especially in the oligotrophic tropical and subtropical oceans (Capone and Subramaniam, 2005; Mahaffey *et al.*, 2005). *Trichodesmium* forms extensive surface blooms that stimulate the biogeochemical cycling of carbon and nitrogen in an area corresponding to almost half of the Earth's surface (Davis and McGillicuddy, 2006; Carpenter and Capone, 2008).

The impacts of enhanced pCO_2 on *Trichodesmium* IMS101 have been actively investigated. Increased pCO_2 stimulated rates of N_2 fixation and supported higher growth rates and biomass accumulation (Hutchins *et al.*, 2007; Levitan *et al.*, 2007; Ramos *et al.*, 2007). Elevated sea surface temperature (SST) may further extend *Trichodesmium's* spatial distribution and hence its importance in the nitrogen cycle at higher latitudes (Breitbarth *et al.*, 2007). Preliminary studies show further enhancement of N_2 fixation and growth under combined high pCO_2 and warmer temperatures (Hutchins *et al.*, 2007). Yet, to our knowledge, the mechanisms underlying these phenomena are unknown.

Nitrogen fixation is expensive, requiring substantial investments in cellular energy, reductant and material resources. Cyanobacterial diazotrophs must separate the antagonistic processes of N_2 fixation and oxygenic photosynthesis to avoid the inhibition of the nitrogenase enzyme by oxygen. Moreover, photosynthetic carbon fixation supplies organic skeletons as substrates for nitrogen assimilation. In many aquatic photosynthesizing organisms intracellular carbon concentrating mechanisms

© 2010 Society for Applied Microbiology and Blackwell Publishing Ltd

(CCM) provide and maintain adequate CO_2 concentrations around RubisCo, thus mitigating limitations due to the generally low availability of ambient CO_2 (aq) in seawater (Raven, 1997; Tortell *et al.*, 2000; Badger *et al.*, 2006).

Genomic analysis of *Trichodesmium* (http://genome.jgi-psf.org/finished_microbes/trier/trier.home.html) reveals that *Trichodesmium* IMS101 lacks known high affinity uptake complexes for Ci, suggesting that *Trichodesmium* IMS101 might respond strongly to changes in pCO_2. Yet, *Trichodesmium* IMS101 uses the abundant HCO_3^- in seawater for over 90% of its inorganic carbon uptake under varying pCO_2 concentrations (Kranz *et al.*, 2009). Considering the steady availability of its major dissolved inorganic carbon (DIC) source, HCO_3^-, under projected pCO_2 levels, it is surprising that *Trichodesmium* responds to an increase in pCO_2 with enhanced N_2 fixation and growth (Levitan *et al.*, 2007).

N_2 fixation is regulated at the transcriptional, post-transcriptional and post-translational levels (Capone *et al.*, 1990; Zehr *et al.*, 1993; Chen *et al.*, 1998; 1999). Nitrogenase synthesis and activity in *Trichodesmium* spp. typically exhibit a diel cycle, with nitrogenase activity confined to the photoperiod by a complex spatial and temporal strategy that allows nitrogenase and photosynthesis to operate concurrently during the photoperiod (Lin *et al.*, 1998; Chen *et al.*, 1999; Mulholland and Capone, 1999; Berman-Frank *et al.*, 2001a; Küpper *et al.*, 2004).

The highest rates of N_2 fixation occur around midday in parallel with peak mRNA transcript abundance for *nifH,* the gene encoding the Fe protein subunit (NifH) of the nitrogenase (Chen *et al.*, 1999). The nitrogenase holoenzyme is synthesized each morning via an increase in the expression of the *nifHDK* operon (Capone *et al.*, 1990; Chen *et al.*, 1998). The assembly of nitrogenase is complex, involving the products of the core subunit *nifHDK* genes along with products from additional genes located within the *nif* operon (Raymond *et al.*, 2004). Nitrogenase comprises two subunits, the MoFe dinitrogenase protein and the dinitrogenase reductase Fe protein, which are encoded by the *nifHDK* operon (Zehr *et al.*, 1991). The MoFe protein is a tetramer of two NifD (α) and two NifK (β) subunits. The $\alpha\beta$ pairs are functionally equivalent dimers, each of which binds molecular nitrogen and reduces it to ammonia. The Fe protein, also called the nitrogenase reductase, is the obligate electron donor to the MoFe protein, and is a homodimer formed by two NifH (γ) subunits. The Fe protein is synthesized and degraded daily, with the levels of active NifH protein corresponding roughly to nitrogenase activity (Zehr *et al.*, 1993). The metabolic signals causing the modification and concomitant activation of the *nifH* gene and the nitrogenase protein biosynthesis are not yet known (Zehr *et al.*, 1993; Mulholland and Capone, 2000).

The NH_4^+ generated by nitrogenase activity in *Trichodesmium* spp. is assimilated via the glutamine synthetase/glutamate synthase (GS/GOGAT) pathway (Carpenter *et al.*, 1992; Kramer *et al.*, 1996; Mulholland and Capone, 2000). In field samples of *T. thiebautii*, glutamine synthetase (GS) transcript levels increased to a maximum in the afternoon during the period of maximum N_2 fixation (Kramer *et al.*, 1996), while GS activity remained steady throughout the diel cycle (Carpenter *et al.*, 1992). A positive correlation between the abundance of GS protein and the nitrogenase enzyme was observed in *Trichodesmium* spp. (Carpenter *et al.*, 1992). Moreover, GS was suggested to play an important regulatory role in N_2 fixation either directly or indirectly, by preventing feedback inhibition from accumulated metabolites (Flores and Herrero, 1994; Mulholland and Capone, 2000).

Diazotrophs, especially non-heterocystous diazotrophs such as *Trichodesmium* spp., are metabolically and ecologically restricted by the direct and indirect energetic demands of N_2 fixation. Moreover, the complexity of the co-occurring energy producing processes of photosynthesis and respiration, and the energy consuming processes of CCM, carbon fixation, anti-oxidant activities and N_2 fixation, require tight coupling and regulation of energy and resource allocation. Accordingly, these resources may be reallocated and their regulation modified (Levitan *et al.*, 2007) to allow for the higher N_2 fixation and growth rates demonstrated at higher pCO_2 and temperatures in *Trichodesmium* (Hutchins *et al.*, 2007).

To elucidate the mechanisms underlying *Trichodesmium's* response to the combined changes in pCO_2 and temperature, we grew *Trichodesmium* IMS101 at varying pCO_2 (250, 400 and 900 μatm pCO_2) and temperatures (25°C and 31°C), and examined key metabolic processes and diel changes in transcript, protein and activity levels related to nitrogen fixation and assimilation.

Results

Growth rates and C, N, P stoichiometry

Temperature and pCO_2 co-affected the cultures, with 900 μatm/31°C cultures having the highest growth rates, consistent with previous studies (Hutchins *et al.*, 2007; Levitan *et al.*, 2007). In cultures grown at 400 μatm/25°C (control treatment) the growth rates were 0.17 ± 0.04 day^{-1}. Growth rates increased by 51% under 250 μatm/31°C relative to the control but were not significantly different according to Scheffe *post hoc* test. The temperature contribution yielded a significant increase of growth rates and increased by 58% under 400 μatm (reaching 0.27 ± 0.01 d^{-1}). Both 900 μatm acclimations were significantly different from the control. At 31°C the increase in

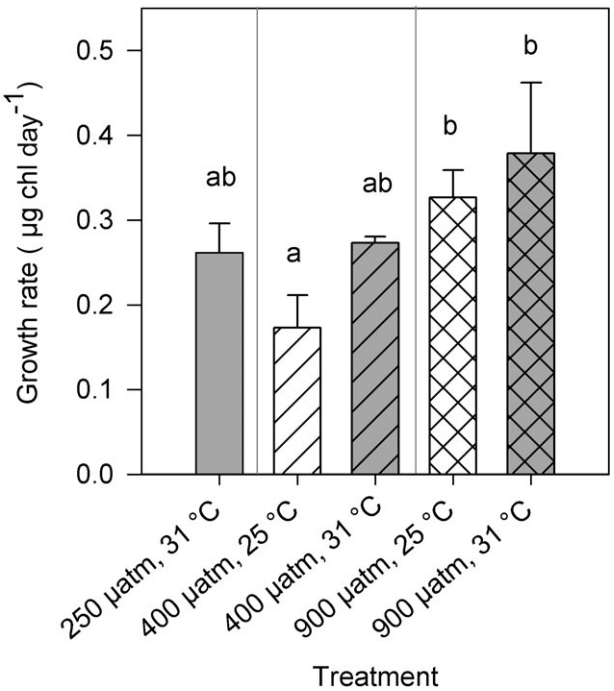

Fig. 1. Exponential growth rates of *Trichodesmium* IMS101 under a matrix of pCO_2 (250, 400 and 900 µatm) and temperatures (25°C and 31°C). Open bars: 25°C, grey bars: 31°C. Values represent treatment average ($n = 3$ or 4). Errors are ±1 standard deviation. Average values are significantly different according to both Kruskal–Wallis Test ($p < 0.05$) and to one-way ANOVA ($p < 0.05$). Different letters represent significant difference between groups according to Scheffe *post hoc* test.

growth rates between 400 and 900 µatm was 15% (from 0.33 ± 0.03 to 0.38 ± 0.08) but was not entirely significant (Fig. 1).

We did not resolve distinct patterns in the cellular stoichiometry of C, N or P during the photoperiod (data not shown) for any of the treatments. C : N values were significantly different between the control and the 250/31°C and 900/31°C treatments (one-way ANOVA, $p < 0.05$, Scheffe *post hoc* test). However, the mean C : N ratio for all samples was 6.53 ± 0.75 ($R^2 = 0.91$, $n = 61$, Fig. 2A). Although the data exhibited partially significant differences among the treatments, this was due to statistical test on a large number of independent replicates, and is not physiologically meaningful. The mean value of 6.53 ± 0.75 approximates the 6.6 (Redfield) C : N ratio and accords well with literature values of 5.6 ± 0.35 for cultured *Trichodesmium* across a range of steady-state growth rates (Holl and Montoya, 2008) and with the 4.7–7.3 range reported by LaRoche and Breitbarth (2005).

While C : N remained relatively constant, the cellular C : P ratios varied significantly between treatments (one-way ANOVA, $p < 0.05$, Scheffe *post hoc* test). All cultures were grown at replete P concentrations, yet

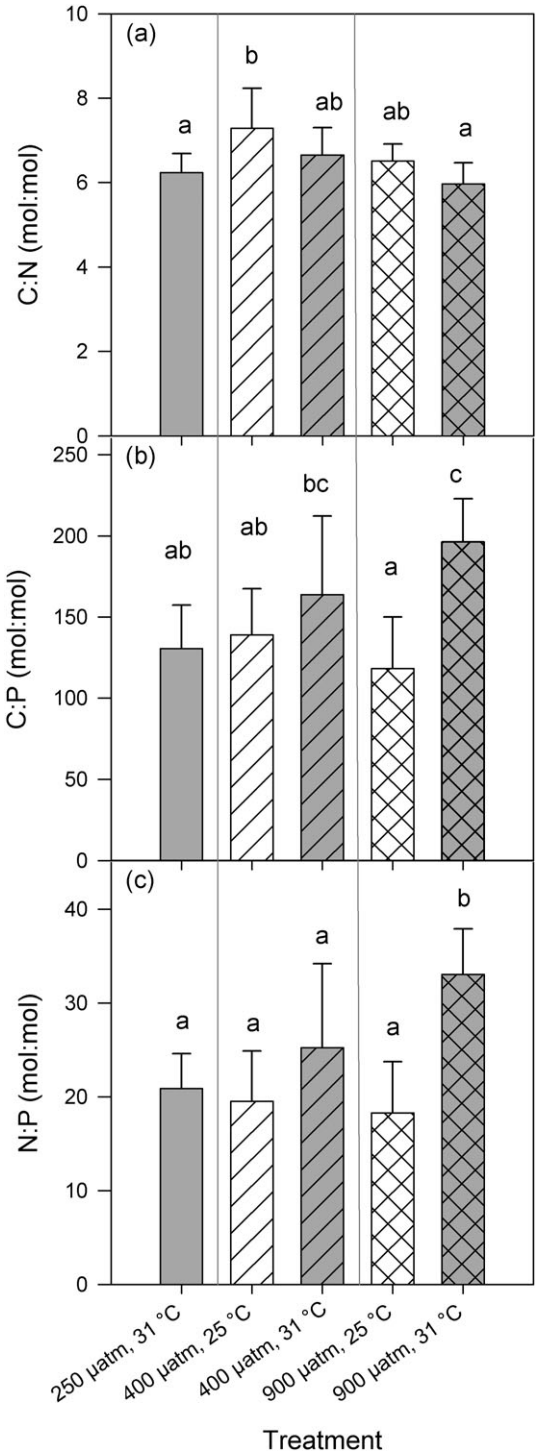

Fig. 2. Stoichiometric composition (mol : mol) of *Trichodesmium* IMS101 under a matrix of pCO_2 and temperatures. (A) Carbon: Nitrogen (C : N) ratio, (B) Carbon: Phosphorus (C : P) ratio and (C) N : P ratio. Open bars: 25°C, grey bars: 31°C. Stoichiometric ratios are presented by treatments ($n = 12$–13). Errors are ±1 standard deviation. Significance between groups was determined by one-way ANOVA ($p < 0.001$) followed by a Scheffe *post hoc* test. According to Scheffe *post hoc* test $p < 0.001$ for C : N averages, $p < 0.05$ for C : P averages and $p < 0.001$ for N : P averages. Different letters represent significant difference between groups.

C : P ratios exhibited temperature dependency at both 400 and particularly at 900 μatm (Fig. 2B). Cultures grown at 400 μatm increased their C : P ratio by 18% (from 139 ± 28 at 25°C to 167 ± 48 at 31°C) with the increase of temperature. The impact of temperature on elemental stoichiometry of C : P was more pronounced under 900 μatm, where elevated temperatures significantly increased the C : P ratio by 66% (from 118 ± 32 at 25°C to 196 ± 27 at 31°C, mol : mol) (Fig. 2B). Only the N : P ratios of our 'greenhouse' (900 μatm/31°C) treatment were significantly higher (~33) than all others (one-way ANOVA, $p < 0.05$, Scheffe *post hoc* test), where the N : P values were closer to the Redfield ratio of 16.

N_2 fixation – transcript level, protein abundance and nitrogenase activity

We examined the Fe protein of the nitrogenase at different levels: the *nifH* mRNA transcript levels, the NifH protein subunit abundance, and the enzymatic activity of the nitrogenase at several points during the photoperiod (Fig. 3).

The diel trends in the mRNA transcript levels were influenced by pCO_2 levels. For comparisons of the *nifH* enrichment factor across growth treatments and measurement times (in Fig. 3A), we normalized transcript levels to the value of the early morning measurements of the ambient, 400 μatm/25°C treatment (control). Under low (250 μatm) and ambient (400 μatm) pCO_2, at both 25°C and 31°C, the *nifH* transcripts abundance followed the typical diel activity pattern of N_2 fixation for *Trichodesmium* (as presented in Fig. 3C) with a maximum abundance matching the midday peak in N_2 fixation rates. At high pCO_2 (900 μatm) this typical midday peak was shifted earlier, with *nifH* mRNA measured abundance highest at 1 h into the photoperiod and declined thereafter (Figs 3A and 4A). For all treatments, transcript levels declined to minimal levels by the end of the photoperiod.

Nitrogenase enzyme abundance, estimated by quantitative immunodetection of the NifH subunit of the Fe protein (Fig. 3B), followed a diel trend in the 31°C cultures, similar to that previously found for the NifD subunit of the MoFe protein (Chen *et al.*, 1998). We did not resolve a diel trend for NifH protein abundance in the 25°C cultures, despite a strong diel pattern in nitrogen fixation (Fig. 3C). At the height of N_2 fixation, from 5 to 9 h of the photoperiod, NifH protein abundance was approximately 274 ± 96 pmol μg total protein^{-1}, $n = 13$ across all growth treatments, irrespective of the differences in nitrogenase activity.

Nitrogenase activity was measured using the acetylene reduction assay as a proxy for nitrogen fixation (Fig. 3C). Consistent with previous observations (Hutchins *et al.*,

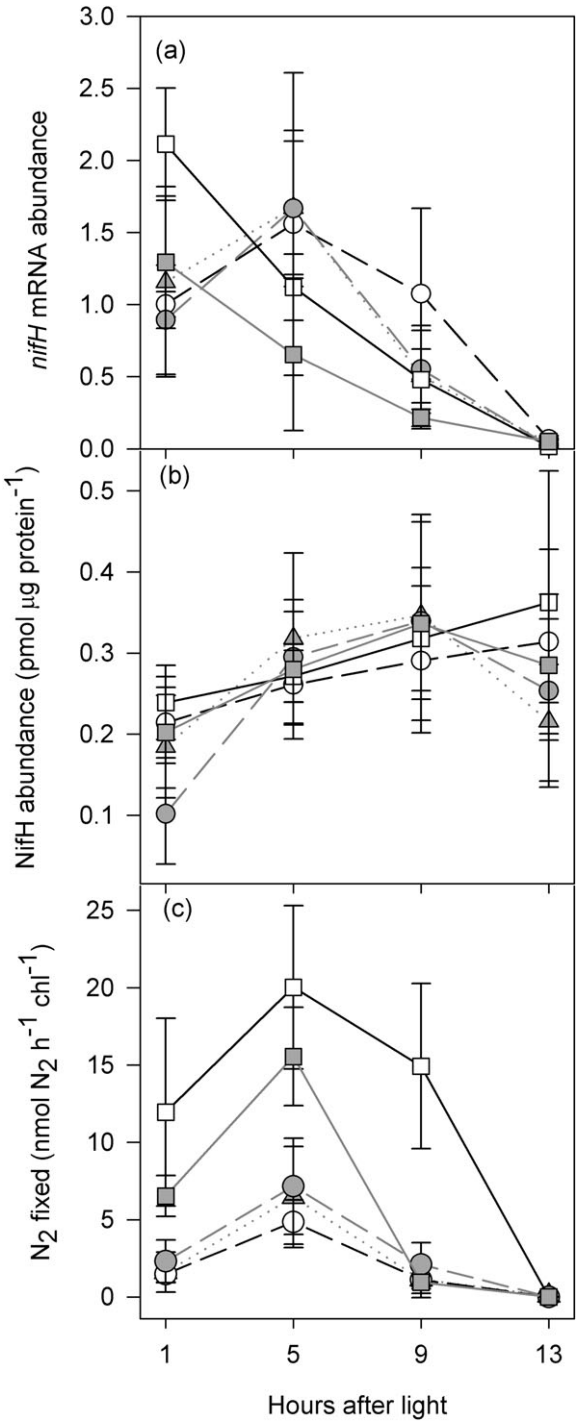

Fig. 3. Temporal changes in *nifH*, NifH and nitrogen fixation for *Trichodesmium* IMS101 under a matrix of pCO_2 and temperatures. A. *nifH* mRNA transcript levels estimated according to the $2^{-\Delta\Delta Ct}$ method, with 16s rRNA as the endogenous reference gene and the ΔCt values of the GOI from the control treatment at 1 h after illumination, as the calibrator.
B and C. (B) NifH protein amount (pmol μg total protein^{-1}) and (C) Rate of N_2 fixation (nmol N_2 fixed h^{-1} μg chl^{-1}). Open symbols and black lines are for 25°C, grey symbols and grey lines represent 31°C. Squares: 900 μatm pCO_2; circles: 400 μatm pCO_2; triangles: 250 μatm pCO_2. $n = 3$ for all. Errors are ±1 standard deviation.

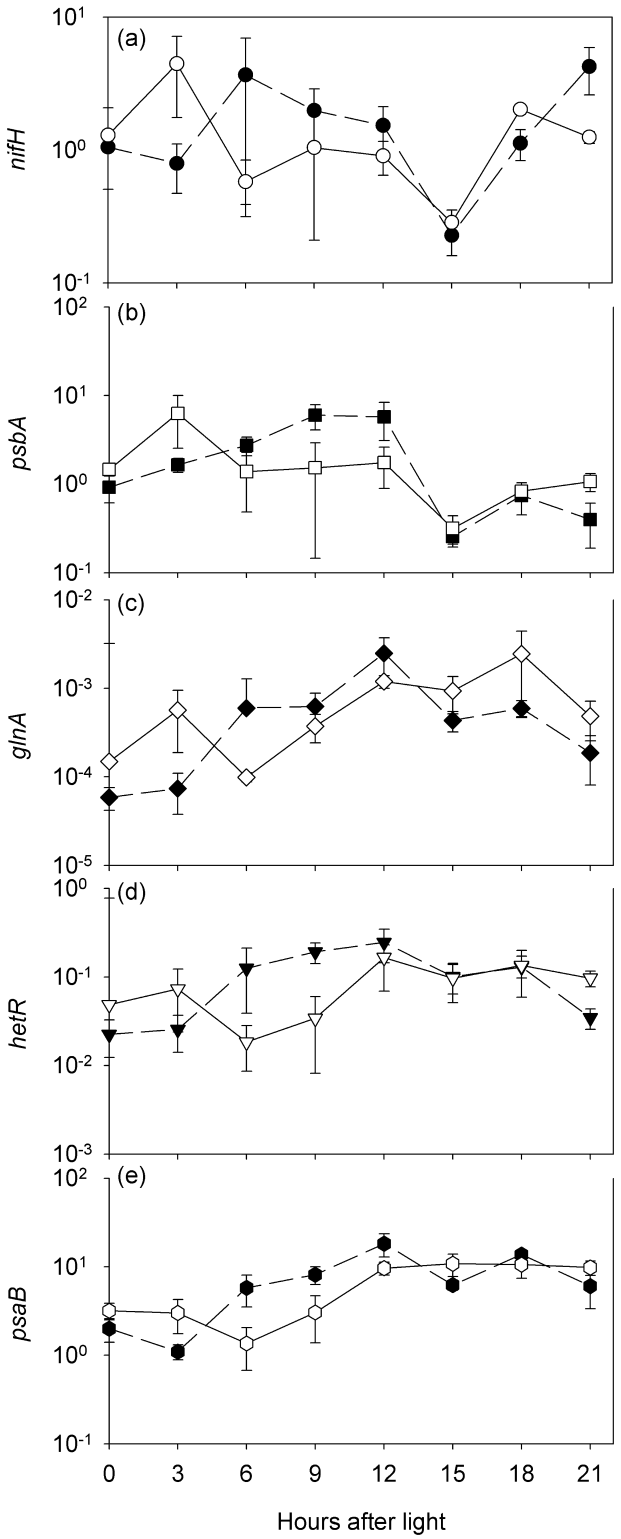

Fig. 4. Diel cycles of mRNA transcripts of five genes for *Trichodesmium* IMS101 under 400 μatm pCO_2 and 900 μatm pCO_2 (both under 25°C). (A) *nifH*, encodes for Fe protein of nitrogenase, (B) *psbA,* encodes for D1 subunit of photosystem I, (C) *glnA,* encodes for glutamine synthetase, (D) *hetR* encodes a key element in cyanobacteria nitrogen related metabolism, and is involved in regulation of heterocysts, and in nitrogen fixation pathways in *Trichodesmium*, (E) *psaB* encodes for a photosystem I subunit. Black symbols and dash lines – 400 μatm, open symbols and solid lines – 900 μatm. Relative abundance estimated according to the $2^{-\Delta\Delta CT}$ method, with 16S rRNA as the endogenous reference gene, and average ΔCt values of the *nifH* from the 400 μatm /25°C treatments as a calibrator. Note the different scale on the *y*-axes. $n = 3$ for all. Errors are ±1 standard deviation.

2007; Levitan *et al.*, 2007; Ramos *et al.*, 2007), nitrogenase activity was two- to fivefold higher in the 900 μatm pCO_2 treatments than at 400 and 250 μatm pCO_2. For all treatments, nitrogen fixation followed a clear diel pattern, with maximum fixation occurring approximately 5 h into the photoperiod (Chen *et al.*, 1998; Berman-Frank *et al.*, 2001a). In agreement with our previous work, elevated pCO_2 increased N_2 fixation rates, although no significant changes were observed between the low and ambient pCO_2 acclimations (250 μatm and 400 μatm pCO_2) (Levitan *et al.*, 2007). The increase in temperature did not significantly increase N_2 fixation rates. During the peak of N_2 fixation (5 h into the photoperiod), fixation rates increased from values of 4–7 nmol N μg chl^{-1} h^{-1} at the low and ambient pCO_2 acclimations (250 μatm and 400 μatm pCO_2) to 15–20 nmol N_2 μg chl^{-1} h^{-1} for both 900 μatm acclimations.

In *Azotobacter vinelandii*, each dinitrogenase unit can fix 1 N_2 to 2 NH_4^+ in 1.5 s (Vichitphan, 2001). Based on the similarity between *Trichodesmium's* nitrogenase and that of *Azotobacter vinelandii* (Zehr *et al.*, 1997), we expressed this turnover time, under an assumption of a cellular stoichiometry of 6NifH:2NifDK, as measured in *Gloeothece* strain ATCC 27152 (Reade *et al.*, 1999). Using this stoichiometry of 6NifH:2NifDK, the minimum reaction rate can be expressed as of 0.44 NH_4^+ s^{-1} $NifH^{-1}$. An alternate assumption of the minimum stoichiometry of 4NifH:2NifDK, based on enzyme structural data that reveal two docking sites for the Fe protein on the FeMo protein, generates a maximum reaction rate of 0.67 NH_4^+ s^{-1} $NifH^{-1}$ [1N_2 to 2NH_4^+ 1.5 s^{-1} $(2NifH)^{-1}$]. These alternative values are indicated with dotted lines in Fig. 5 to show an approximate range for potential nitrogenase reaction rates (Fig. 5).

We then normalized N_2 fixation rates to NifH protein abundance to estimate NifH apparent reaction rates (Fig. 5), and compared these calculated rates to the range of the potential nitrogenase reaction rates. By doing so, we assumed a constant Fe protein : FeMO protein ratio, based on the range provided by Reade and colleagues (1999). pCO_2 concentrations appeared to control the apparent reaction rates with peak N_2 fixation in the middle of the light period averaging from 0.42 to 0.47 NH_4^+ s^{-1} $NifH^{-1}$ under 900 μatm pCO_2 31°C and 25°C respectively (Fig. 5). An exception was observed in the 9 h time point

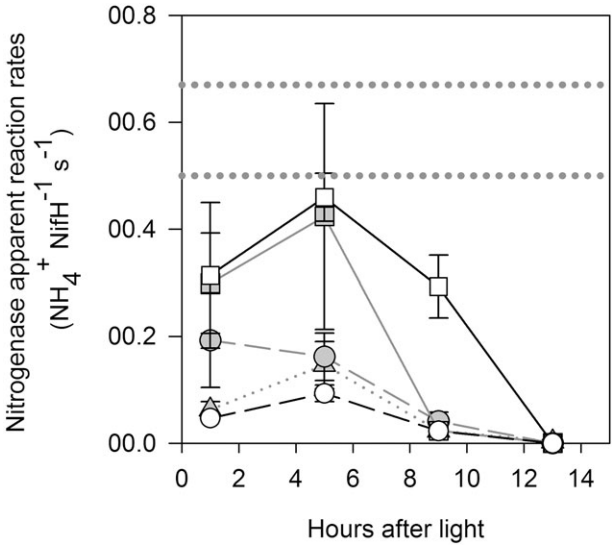

Fig. 5. Temporal changes in the apparent reaction rate of nitrogenase in *Trichodesmium* IMS101, under a matrix of pCO_2 and temperatures. The horizontal region between the dotted lines represents the nitrogenase potential reaction rate range based on published literature from other species, presented for comparison with the apparent reaction rates estimated for *Trichodesmium* IMS101. Open symbols and black lines are for 25°C, grey symbols and grey line represent 31°C. Squares: 900 pCO_2; circles: 400 μatm pCO_2; triangles: 250 μatm pCO_2. $n = 3$ for all. Errors are ±1 standard deviation.

for 900 μatm, in which the 25°C acclimation exhibited higher N_2 fixation rates. Our calculations show that at high pCO_2, cultures performed at ~80–100% of the nitrogenase reaction rates from published literature, while the apparent enzymatic reaction rates for low and ambient CO_2 cultures were much lower, ranging from 13% to 38% of the nitrogenase reaction rates (taking 0.44–0.67 NH_4^+ s^{-1} $NifH^{-1}$ as the nitrogenase potential range).

Transcription patterns

Our observations (Figs 1–5) show that nitrogen metabolism in *Trichodesmium* IMS101 is influenced by changes in pCO_2 to a much greater extent than by the 6 degree temperature increase. Accordingly, we extended the experiments presented in Fig. 3A and examined in detail the diel expression of several key genes in cultures growing under 400 μatm/25°C pCO_2 and under 900 μatm /25°C pCO_2 (Fig. 4) using RT-qPCR. Transcripts were obtained from matched primer pairs designed for *nifH*, *psbA*, *glnA*, *hetR* (Fig. 4D) and *psaB* (Table 1).

Our results show that *Trichodesmium* IMS101 cultures, grown for several months under elevated pCO_2, changed their mRNA expression patterns for several key genes involved in nitrogen metabolism and photosynthesis. The differences between the pCO_2 treatments were not reflected in the relative abundance of the genes themselves (using average of *nifH* at 400 μatm as a calibrator), resulting in the same enrichment factors for each gene under both pCO_2 levels (Fig. 4A–E). However, when comparing the relative abundance among the five genes, it is noticeable that while the transcript abundance of *nifH*, *psbA* and *psaB* (Fig. 4A, B and E) is similar, the relative abundance of *hetR* and *glnA* (Fig. 4C and D) is 1–2 and 3–4 orders of magnitude lower, respectively (Fig. 4, note the differences in the y axes scale). Although sampled from two independent experiments, the nifH transcript patterns shown in Figs 3A and 4A correspond to the same time points and show similar trends.

Typically, and in agreement with previous studies at ambient pCO_2 (i.e. Chen *et al.*, 1999), levels of all the transcripts remained relatively low from 0–3 h after the onset of light at 400 μatm pCO_2. From 3 h after light induction, the transcript levels increased, with specific peaks for each gene. The first gene transcript to peak was *nifH* at 6 h after the onset of light (Fig. 4A), followed by *psbA* at 9 h (Fig. 4B) and *glnA* and *psaB* at 12 h after light (Fig. 4C and E). *nifH, psbA* and *psaB* exhibited additional peaks. *nifH* peaked again 3 h before the onset of light, while the *psBa* and *psaB* transcripts increased slightly 6 h before light. At 900 μatm pCO_2 *nifH*, *psbA* and *glnA* transcript levels (Fig. 4A–C) increased at the start of the photoperiod and peaked concurrently 3 h into the photoperiod. At this pCO_2 acclimation, *hetR and psaB* transcript levels were highest towards the beginning of the dark phase and were relatively steady throughout the dark phase (Fig. 4D and E). Thus, when comparing both growth conditions, the main impact of acclimation at 900 μatm pCO_2 was a more synchronized expression of all genes tested, with an obvious peak at 3 h into the photoperiod (Fig. 4A–E).

Table 1. Sequences of forward and reverse primers for five target genes, *nifH*, *glnA*, *psbA*, *psaB* and *hetR*.

Gene	Description	Forward primer (5′ to 3′)	Reverse primer (5′ to 3′)
nifH	Fe protein of nitrogenase	GGTCCTGAGCCTGGTGTAGG	GATAGCAGTAATAATACCACGGCCA
glnA	Glutamine synthetase	AATTTGGAAAGACGGAGAGCC	AAATTAGCATAACCATCACCCCAG
psbA	Subunit of photosystem II (D1)	CAGCGGTCGCGTAATCAAT	CATTCCTAAGTTAGCGCGGTTAA
psaB	Subunit of photosystem I	TCGGATCTGGTATGGAATTGC	CCATCGTGGGTTTCAAAGTCAT
hetR	Key regulatory gene in heterocyst differentiation	TTATATAATGGTTGAAGATACAGCTCGC	CCAGTCCTTCATTAACCGGAAA

Primers were designed using Primer Express Software v2.0.

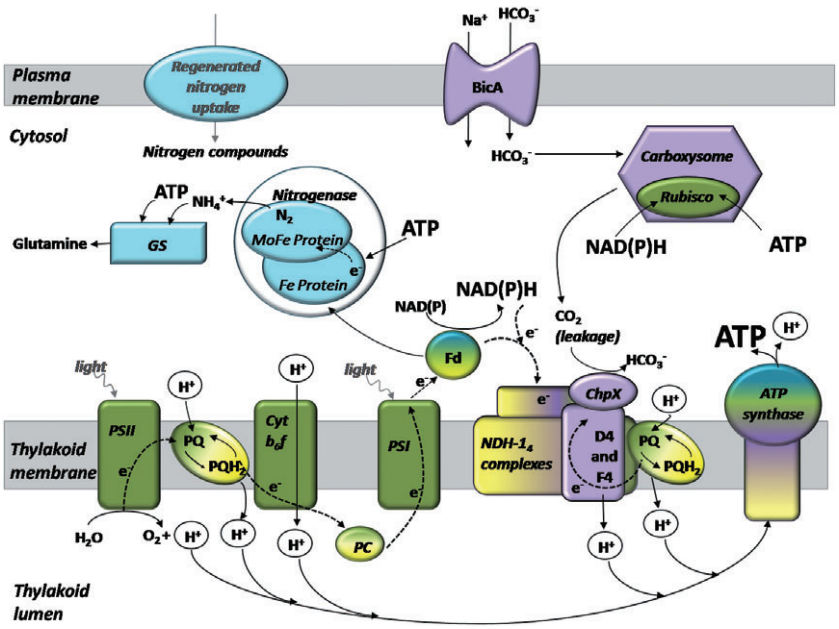

Fig. 6. Schematic representation of major cellular complexes involved in energy flow [electron, ATP, NAD(P)H] and organic skeletons in *Trichodesmium* IMS101. We suggest that reallocation of energy between these components allows for increased N_2 fixation and growth rates elevated high pCO_2. BicA and NDH-1_4 complexes are after Badger and Price (2003) and Badger and colleagues (2006). Photosynthetic complexes are green, respiratory contribution is marked by yellow, CCM complexes are purple and nitrogen metabolism is represented in blue. The shared metabolic components are indicated by a mix of the respective colours above.

Discussion

We examined the combined effect of high pCO_2 and elevated temperatures on the diazotroph *Trichodesmium* IMS101 at the transcriptional, translational and enzymatic activity levels. Our results corroborate earlier studies showing enhanced growth (Fig. 1) and N_2 fixation rates (Fig. 3C) under higher pCO_2 (Hutchins *et al.*, 2007; Levitan *et al.*, 2007; Ramos *et al.*, 2007). Additionally, we show that while higher temperatures combined with elevated pCO_2 further stimulated growth rates, nitrogenase activity increased under elevated pCO_2, independently of temperature changes (except 9 h after light, Figs 3C and 5).

The cellular stoichiometry of carbon and nitrogen reflected in the C : N ratios (Fig. 2A) remained relatively stable across all growth conditions tested. C : N values approximated the Redfield ratio (6.53 $\pm$ 0.75, $n = 61$) and corresponded with published studies (Berman-Frank *et al.*, 2001b; LaRoche and Breitbarth, 2005; Küpper *et al.*, 2008), including studies showing the effects of pCO_2 on *Trichodesmium* (Hutchins *et al.*, 2007; Levitan *et al.*, 2007; Ramos *et al.*, 2007; Kranz *et al.*, 2009). The relatively stable C : N ratios at different pCO_2 levels, combined with the apparent constancy in photosynthetic rates (Levitan *et al.*, 2007; Kranz *et al.*, 2009), suggest that net nitrogen and carbon accumulation in the cell remains proportional under both ambient (400 µatm) and high (900 µatm) pCO_2. For exponentially growing *Trichodesmium* NIBB1067 cultures (another strain of *T. erythraeum*), under comparable conditions, N_2 fixation accounted for only 14–16% of the gross daily N uptake, under comparable conditions (Mulholland *et al.*, 1999). Hence, growth under elevated pCO_2 may increase the fraction of assimilated organic nitrogen generated by N_2 fixation (per day), rather than change the net amount of cellular nitrogen accumulated in the cell.

In contrast with the relative stability found for carbon and nitrogen, *Trichodesmium* spp. exhibit highly flexible phosphorus quotas. *Trichodesmium* IMS101 C : N : P ratios may reach $C_{(585\pm56)} : N_{(90\pm10)} : P_{(1)}$ (White *et al.*, 2006), with a plasticity in the N : P ratio that ranges between 11:1 and 125:1 (Krauk *et al.*, 2006). Ratios close to the Redfield ratio were achieved when growing in P replete media, probably due to phosphorus luxury uptake (White *et al.*, 2006). Our results demonstrate higher C : P in *Trichodesmium* IMS101 grown at enhanced temperatures and higher pCO_2 (Fig. 1). This suggests that less P is required for supporting higher N_2 fixation and growth rates in *Trichodesmium* IMS101 under 'greenhouse' conditions.

What mechanisms can account for the stoichiometric stability of carbon and nitrogen, yet enable higher N_2 fixation rates, elevated C : P, and increased growth rates under the predicted temperatures and elevated pCO_2? We explored protein abundance and mRNA transcript levels to understand the regulation of nitrogen metabolism. We focused on two important protein subunits, NifH (nitrogenase Fe protein) and GlnA (a subunit of glutamine synthetase) that assimilates the recently fixed NH_4^+ to organic compounds via the GS/GOGAT pathway. The mobile subunit of the nitrogenase, the Fe protein (Fig. 6), functions as a link between the metabolic electron donors (Fd, NADPH) and the N_2 reducing subunit, the MoFe protein (Zehr *et al.*, 1997; Raymond *et al.*, 2004). The NH_4^+ generated via nitrogenase is volatile and toxic and

so GS activity closely follows nitrogenase activity (Mulholland and Capone, 2000). For all pCO_2/temperature combinations, the NifH abundance (pmol μg protein^{-1}) was similar during the peak of N_2 fixation (Fig. 3b). GlnA subunit abundance was also stable during the day and across treatments (data not shown).

While NifH and GlnA protein pools did not notably change between treatments, we attempted to calculate an estimated reaction rate for nitrogenase (Fig. 5). Based on our assumptions and calculations, higher pCO_2 can increase the estimated nitrogenase reaction rates (Fig. 5). This may indicate differential sensitivity of enzymatic function to environmental conditions. While elevated pCO_2 may enable higher enzymatic activities that are closer to the published potential nitrogenase reaction rates for other prokaryotes, the experimental range of temperatures here does not seem to affect it.

We observed that at 400 μatm *glnA* transcripts increased during the light phase and reached maximum levels before the end of the photoperiod, 6 h after the peak in *nifH* transcripts abundance (Fig. 4A and 4C). This corresponds with previous observations done on field samples of *Trichodesmium thiebautii* demonstrating two peaks of GS mRNA transcript abundance, one before dawn (that we did not observe) and the second during late afternoon (Kramer *et al.*, 1996). The diel changes in GlnA transcripts, combined with the relatively small changes in GS activity (Mulholland and Capone, 1999), led to the assumption that *Trichodesmium* spp. possess two GS pools, one of which is a nitrogenase linked pool (Mulholland and Capone, 2000). If the catalytic rate of the GS could be shown to increase under 900 μatm, the increase in the apparent nitrogenase reaction rates (Fig. 5) could further support the assumption that these two enzymes are co-regulated (Flores and Herrero, 1994).

The limited changes in cellular stoichiometry of C : N, the parallel change in C : P ratios and the calculated increased catalytic efficiencies under high pCO_2 led us to further examine the idea of changes in energy allocations of ATP, NAD(P)H, electrons and organic skeletons. In cyanobacteria, including *Trichodesmium*, the metabolic pathways and the cellular currencies (as above) are shared among photosynthesis and CCM, respiration, and nitrogen metabolism (Fig. 6). Based on published literature and our results we suspect that the molecular to physiological changes observed under elevated pCO_2 and temperatures (Figs 1–5) are due to reallocations of these cellular currencies that are environmentally regulated (Fig. 6).

Previously, we hypothesized that changes in pCO_2 will influence photosynthetic rates. However, photosynthetic rates were not significantly modified by pCO_2 (Levitan *et al.*, 2007; Kranz *et al.*, 2009). Therefore, we suggested that high pCO_2 lowers the dependence of *Trichodesmium* IMS101 on energetically expensive active Ci uptake through CCM (Levitan *et al.*, 2007). This allows for greater allocation of ATP, reducing power, and substrates for N_2 fixation and subsequent growth.

While CO_2 is the substrate for RubisCo, many cyanobacteria, including diazotrophs, have carbon concentrating mechanisms (CCM) that enable active uptake and concentration of CO_2 or HCO_3^-, increasing CO_2 concentrations near RubisCo. *Trichodesmium* IMS101 has only a partial suite of CCM genes (Badger *et al.*, 2006). The genes found encode proteins for carboxysomes, homologues of a low affinity high flux HCO_3^- transporter, BicA and a low affinity CO_2 uptake complex, NDH-1_4, while lacking homologues for inducible high affinity Ci uptake systems (Badger *et al.*, 2006). A 'true' functional internal carbonic anhydrase (iCA), required to convert between CO_2 and HCO_3^-, was never found, not in genetic analysis (Badger *et al.*, 2006), nor in lab experiments (S. Kranz and O. Levitan, unpubl. data). The only published study directly measuring CCM activity in *Trichodesmium* (Kranz *et al.*, 2009) demonstrated that *Trichodesmium* IMS101 grown at different pCO_2 levels uses HCO_3^- for over 90% of its DIC uptake, probably via the BicA complex (Fig. 6). Moreover, elevated pCO_2 resulted in a decrease in the cellular affinity to total DIC but not in the carboxylation efficiency of RuBisCo (Kranz *et al.*, 2009).

Although principally a bicarbonate user, *Trichodesmium* IMS101 possesses NDH-1 dehydrogenase (NDH-1_4). The NDH-1_4 is restricted to the thylakoid membrane in cyanobacteria (Ohkawa *et al.*, 2001; Badger *et al.*, 2006, Fig. 6) and is probably involved in the hydration that converts CO_2 to HCO_3 (Price and Badger, 2002). This provides further evidence linking CCM to both photosynthetic and respiratory electron chains and to the thylakoid membrane potential (Fig. 6). Neither BicA nor NDH-1_4 directly consumes ATP (Badger *et al.*, 2006). Yet, BicA is strongly dependent on photosynthetic electron flow required to maintain the transmembrane potential that drives the Na^+/HCO_3^- exchange (Kranz *et al.*, 2009, S. Kranz and O. Levitan, unpubl. data and Fig. 6), while NDH-1_4 is coupled to electron flow (Badger and Price, 2003).

NADPH and reduced ferredoxin (Fd, Fig. 6) can act as potential electron donors for both NDH-1_4 and nitrogenase Fe protein. We propose that more efficient proton pumping into the thylakoid lumen via the NDH-1_4 may be possible through coupling with Q cycle activity (Badger and Price, 2003; Milligan *et al.*, 2007), thereby improving the energetics of CO_2 conversion. This can increase the membrane potential and will contribute to the amount of ATP generated by the ATP synthase (Fig. 6). Additionally, lowering the CCM demand for electrons, i.e. via lower affinity to DIC (Kranz *et al.*, 2009), can thereby allow larger electron flux to nitrogenase (Fig. 6). This would

result in an increased electrons flux available for the Fe protein, which could enable increased N_2 fixation rates in areas of limited Fe availability.

Nitrogenase requires at least 16 molecules of ATP to fix one molecule of N_2 into two NH_3 (Postgate, 1998). The Fe protein carries electrons from Fd or NADPH and delivers it to the MoFe subunit, performing a docking, electron transfer, ATP hydrolysis, detach cycle (Hageman and Burris, 1978). Binding of ATP to the Fe protein of the nitrogenase complex (NifH) is essential for the transfer of electrons to the MoFe protein (Hageman and Burris, 1978). The release of the NifH subunit from the MoFe complex, thought to be the rate limiting step in N_2 fixation (Vichitphan, 2001), occurs after the hydrolysis of the bound ATP. ATP could therefore be a limiting substrate for N_2 fixation under 400 and 250 μatm pCO_2.

For nitrogenase, the ATP consumption : electron transfer ratio increases under conditions of nitrogenase enzyme inhibition (Lanzilotta and Seefeldt, 1996; Vichitphan, 2001). At favourable conditions, such as growth at 900 μatm pCO_2, the overall ATP requirement per NH_4^+ generated may decrease (Fig. 6). This could also lead to higher rates of N_2 fixation per nitrogenase, without any substantial changes in the abundance of the nitrogenase Fe subunit (Fig. 3B and C). Lower ATP and Fe requirement per unit of N_2 fixation under elevated pCO_2 could thus enable increased N_2 fixation and growth in areas of limited Fe availability such as found in many oceanic areas (Berman-Frank *et al.*, 2001b; Mills *et al.*, 2004). We therefore propose that acclimation to 'greenhouse' conditions allows for more effective resource utilization.

Transcript abundance does not necessarily directly correspond to protein pools, which in turn can be offset from enzyme activity. Modulation of nitrogenase activity has also been ascribed to a modification of the NifH protein that correlates with a loss of activity late in the light period, following the period of maximum fixation rates (Capone *et al.*, 1990; Zehr *et al.*, 1993; Chen *et al.*, 1998). The large increase in N_2 fixation rates at midday (Fig. 3C) does not correspond with changes in abundance of the NifH protein between the different treatments (Fig. 3B). This may result from either post-translational regulation of the enzyme (i.e. as suggested in Fig. 5) or differences in the abundance of other subunits. Transcription initiation, proteolysis and post-translational modification of the nitrogenase Fe protein could regulate N_2 fixation in *Trichodesmium* IMS101. Although *nifHDK* operon is likely transcribed as a single unit (Dominic *et al.*, 1998), transcription termination upstream of *nifD*, a longer half life of the *nifH* transcript (Chen *et al.*, 1998) or different rates of translation, could result in differential expression of the nitrogenase proteins. *Trichodesmium* IMS101 possesses a circadian clock that controls the expression of the nitrogenase operon and regulates metabolic functions (Chen *et al.*, 1998). Yet, the signal that triggers and controls *nifHDK* gene transcription may be indirect (Chen *et al.*, 1998), for example a change in pCO_2.

We demonstrate that elevated pCO_2, regardless of temperature, impacts transcripts of several genes and protein activity in *Trichodesmium* IMS101. Although the pCO_2 level did not change the relative transcript abundance of the five genes (Fig. 4, note the differences in y axes scales), increased pCO_2 altered *nifH* transcript expression patterns (Fig. 4A) and caused an earlier (3 h after light) peak. This peak was synchronized with the peaks of *psbA* and *glnA* (Fig. 4B and C), and to a lower extent also with *hetR* (Fig. 4D). The relative transcript abundance of the *glnA* and *hetR* was kept notably lower at both pCO_2 (Fig. 4C and D). This corresponds with a fourfold lower abundance of the GlnA protein, of glutamine synthetase, relative to the NifH protein (data not shown).

Utilizing different cellular and mechanistic strategies could enable higher N_2 fixation and increased growth rates under high pCO_2 and temperatures. One strategy is the balance between stoichiometric stability in carbon and nitrogen and the plasticity in P and Fe quotas (Berman-Frank *et al.*, 2001b; 2007; White *et al.*, 2006; Küpper *et al.*, 2008). Phosphorus is a fundamental cellular building block required for ATP, for nucleic acid biosynthesis, and in mediation of post-translational modification that is essential for gene regulation (Scanlan and Wilson, 1999). We suggest that elevated pCO_2 allows for lower P quotas and reduced bioenergetic demands, i.e. CCM, relative to C (Fig. 2B). This, in turn, can enable higher N_2 fixation and increased growth rates (Figs 1 and 3C). A second strategy for achieving higher growth rates is to lower the energetic investment in building protein complexes. If verified, an increase in the apparent reaction rates of nitrogenase (Fig. 5) and possibly GS, with no increase in NifH protein (Fig. 3B) or GlnA amount (data not shown), could account as an example for this strategy at higher pCO_2.

Trichodesmium is an ancient diazotrophic cyanobacterium that evolved during the Archaean (Berman-Frank *et al.*, 2001a) and thrives in the present oceans, forming huge blooms easily observed by satellites over the subtropical and tropical oceans (Capone *et al.*, 1997; Capone and Subramaniam, 2005). *Trichodesmium's* arsenal of cellular and mechanistic strategies, including the combination of energy reallocation (Fig. 6), flexibility of the CCM operation (Kranz *et al.*, 2009, S. Kranz and O. Levitan, unpubl. data) and P stoichiometry (Fig. 2) together with possible improved enzymatic efficiency (Figs 3C and 5), will enable higher N_2 fixation and growth at higher pCO_2 and temperatures, while requiring less P, and possibly less Fe, per C. We suggest that this will extend *Trichodesmium's* potential niche and allow the persistence and dominance of this cyanobacterium in the future oceans,

including tropical areas where it is presently scarce (Church *et al*., 2008; Bonnet *et al*., 2008; 2009).

Experimental procedures

Culturing and growth

Trichodesmium IMS101 stock cultures were grown in YBCII medium (Chen *et al*., 1996) at 25°C, 12:12 light/dark cycle at ~80 μmol photons m^{-2} s^{-1} white light and near future ambient pCO_2 concentrations of 400 μatm pCO_2. Diluted batch cultures were grown in sterile square 1 L Nalgene bottles as single filaments with gentle bubbling that was sufficient to prevent formation of aggregates but did not cause high turbulence that could harm the integrity of the filaments. Stock cultures were unialgal and under exponential growth the bacterial biomass was negligible and was not observed under light microscopy.

For experiments, cultures were enriched with the appropriate air and CO_2 mix for at least 1.5–2 months by bubbling. While acclimation time changes for different species, it is generally assumed that growth under the required conditions for > 10 generations of growth are sufficient (MacIntyre and Cullen, 2005).

We applied the following pCO_2 concentrations: ~250 μatm (pre-industrial pCO_2 concentration), ~400 μatm (near future ambient) pCO_2 and ~900 μatm (expected 2100) pCO_2 level. The temperatures used for the experiments were 25°C and 31°C. Acclimation of stock culture to the experimental temperatures was done by a gradual increase of 1°C a week. The pCO_2 input to the cultures was continuously monitored using an EMP-SB4-TX CO_2 gas analyser (Emproco, Ashkelon, Israel). The 400 μatm/25°C treatment was our control since the current ambient pCO_2 in the atmosphere in oceanic regions is ~400 μatm and 25°C is within the range of temperature distribution for natural populations of *Trichodesmium* spp. (20–30°C) found in the environment. Growth rates were determined on the basis of chlorophyll *a* (μg ml^{-1}). Biomass was kept under 0.2 μg chl ml^{-1}, thereby maintaining a low enough biomass that did not additionally influence the carbonate chemistry of the experimental setup.

Chlorophyll a

Cultures were collected on GF/F filters and chlorophyll *a* was extracted by boiling for 6 min in 90% methanol and analysed spectrophotometrically at 664 nm according to Tandeau De Marsac and Houmard (1988).

N_2 fixation

N_2 fixation rates were determined using the standard acetylene reduction assay (Capone, 1993). Cultures aliquots were spiked with acetylene (20% of headspace volume) and incubated for 2 h. Ethylene production was determined on an SRI 310 flame ionization detector (FID)–GC and converted to N equivalents assuming a stoichiometry of 4:1 $C_2H_4 : N_2$ (Capone and Montoya, 2001). Samples of 6.5 ml culture were incubated for 2 h in 15 ml gas tight vials that were later filtered for chlorophyll *a* determination. Chlorophyll *a* per cell did not change significantly between treatments and therefore the results were normalized to chlorophyll *a*.

Elemental stoichiometry

Samples of acclimated, exponentially growing cultures, were taken during 4 time points along the day (1, 5, 9 and 13 h after the onset of light) and filtered onto pre-combusted 13 mm GF/F filters. After sampling, the samples were kept in pre-combusted aluminum foil at –20°C and later dried for 24 h at 60°C. Analysis was done using an elemental soil analyser with a thermo conductivity detector (NC 2110, hermoQuest, Waltham, MA, USA) for measuring C and N.

Particulate P was measured following a modified version of the ALOHA protocol (Hawaii Institute of Marine Biology, Analytical Services laboratory at the University of Hawaii). The method relies on the release of organically bound P compounds as orthophosphate, by high-temperature and pressure combustion. The released orthophosphate reacted with a mixed reagent containing sulfuric acid, molybdic acid and trivalent antimony to form phosphomolybdic acid. The solution was reduced to a blue molybdenum complex by ascorbic acid in the mixture, which was then measured spectrophotometrically (880 nm) and calculated using a 12 points standard curve.

Sample collection for protein and RNA

Samples of *Trichodesmium* IMS101 were collected by gentle filtration (in the dark) on polycarbonate filters for both protein (5 μm pore size, 13 mm diameter filters, Osmonics) and RNA (1 μm pore size, 25 mm diameter filters, Osmonics). For both protocols, filtration time was ~1–3 min (due to the low cultures biomass). Filters were placed in sterile DNase and RNase free centrifuge tubes and put directly into liquid nitrogen until transfer to –80°C for storage. Sampling was done at 4 time points during the diel cycle, 1, 5, 9 and 13 h after the onset of light for results presented in Figs 3 and 5. For Fig. 4, sampling was done across a 24 h cycle, every 3 h starting from the onset of light.

Total protein extraction and quantification

Trichodesmium filters were resuspended in 250 μl 1× denaturing extraction buffer, containing 140 mM Tris base, 105 mM Tris–HCl, 0.5 mM ethylenediaminetetraacetic acid (EDTA), 2% lithium dodecyl sulfate (LDS), 10% glycerol, 0.1 mg ml^{-1} PefaBloc SC (AEBSF) protease inhibitor (Roche). Samples were sonicated until thawed with a microtip attachment at a setting of 30% using a Fisher Scientific Model 100 Sonic Dismembrator. To avoid overheating, samples were then refrozen immediately in liquid N_2. Two cycles of freezing followed by thawing by sonication yielded maximal protein extraction with minimal degradation of representative membrane and soluble proteins (Brown *et al*., 2008). Following disruption, samples were centrifuged for 3 min at 10 000 *g* to remove insoluble material and unbroken cells.

The total protein concentration was measured with a modified Lowry assay (Bio-Rad DC) using bovine gamma globulin as a comparative protein standard.

Target protein quantification

Total proteins from samples and quantification standards (AgriSera, Sweden) were separated by electrophoresis on 4–12% acrylamide gradient mini-gels (NuPAGE Bis–Tris gels, Invitrogen) in MES SDS running buffer (Invitrogen) in an XCell Sure-Lock Tank (Invitrogen) at 200 V for 35–60 min. Following electrophoresis the proteins were transferred to polyvinylidene difluoride (PVDF) membranes pre-wetted in methanol and equilibrated in 1× transfer buffer (Invitrogen) using the XCell blot module (Invitrogen) for 60–80 min at 30 V. Immediately following transfer, blots were blocked in 2% ECL Advance blocking reagent (GE Healthcare) in 20 mM Tris, 137 mM sodium chloride pH 7.6 with 0.1% (v/v) tween-20 (TBS-T) for 1 h. For detections of NifH and GlnA, primary antibodies (AgriSera, Sweden) were used at a dilution of 1:40 000 in 2% ECL advance blocking reagent in TBS-T. Blots were incubated in primary antibody solution for 1 h. Blots were incubated for 1 h with horseradish peroxidase conjugated rabbit anti chicken secondary antibody (Abcam), diluted to 1:40 000 in 2% ECL Advance blocking reagent in TBS-T. Blots were developed with ECL Advance detection reagent according to the manufacturer's instructions. Images of the blots were obtained using a CCD imager (DNR, M-ChemiBIS). Protein levels on immunoblots were quantified using Quantity One software (Bio-Rad). Adjusted volume values were obtained and standard curves were used to estimate the amounts of protein in experimental samples (after Brown *et al.*, 2008).

RNA extraction and reverse transcription RT-qPCR

At each sampling time point 30 ml of culture was filtered over 1 μm, 25 mm polycarbonate filter and flash frozen in liquid nitrogen. Samples were stored at −80°C until extraction. mRNA was extracted with the RNeasy Plant Mini Kit (Qiagen Cat. 74904). DNase treatment was accomplished with RNase-Free DNase Set (Qiagen Cat. 79254) as well as with TURBO DNA free (Ambion Cat. AM1907) to erase any DNA contamination. RNA concentration was measured with a NanoDrop ND-1000 Spectrophotometer (peqLab Biotechnologie) and quality was tested with 1% agarose gels. Reverse transcription was conducted with the QuantiTect Reverse Transcription Kit (Qiagen Cat. 205311). RT-qPCR was carried out with Platinum SYBR Green qPCR SuperMix-UDG with ROX (Invitrogen Cat. 11744-500) on an ABI PRISM 7000 Sequence Detection System. Primers for five target genes were designed using Primer Express Software v2.0 (Applied Biosystems) and are presented in Table 1. Transcripts were obtained from matched primer pairs designed for *nifH* (encoding the Fe protein of nitrogenase, Fig. 4A), *psbA* (encoding the unstable D1 subunit of photosystem II, Fig. 4B), *glnA* (glutamine synthetase, Fig. 4C), *hetR* (Fig. 4D) and *psaB* (encoding a photosystem I subunit, Fig. 4E) (Table 1). *hetR* encodes a key element in heterocyst regulation, appears to play an important, although not fully understood, metabolic role in non-heterocystous filamentous cyanobacteria especially after nitrogen depletion (Zhang *et al.*, 2009), and is involved in N_2 fixation pathway in *Trichodesmium* (El-Shehawy *et al.*, 2003).

The RT-qPCR results were checked for inaccurate reactions. Results with deficient primer characteristics and with bad efficiencies according to the LinRegPCR software (Ramakers *et al.*, 2003) were removed prior to calculations. Results were calculated using the $2^{-\Delta\Delta Ct}$ method used to calculate relative changes in gene expression determined from real-time quantitative PCR experiments, according to Livak and Schmittgen (2001). This method examines the threshold cycle (Ct) and indicates the fractional cycle number at which the amount of amplified target reaches a fixed threshold (Livak and Schmittgen, 2001). The Ct values of the gene of interest (GOI) are normalized first to the 16S rRNA gene, which is used here as the endogenous reference gene for each time point. This results in ΔCt values, which are equal to the differences in thresholds for the GOI and the endogenous reference gene (Livak and Schmittgen, 2001). In time-course experiments, the gene expression is often compared internally by normalization with a calibrator, which can be the time zero point. For Fig. 3A we have chosen to use the early morning values of the 400 μatm /25°C samples as a calibrator gene. For Fig. 4 we have chosen the average ΔCt values of the *nifH* from the 400 μatm /25°C treatments as a calibrator, since we wanted to compare the relative abundance of the different genes, as well as their time dependence. The time-dependent patterns of expression found with the normalization to the mean ΔCt values of the *nifH* genes showed the same trends as those obtained with the normalization to the initial control time point. Results and statistics are presented according to Bustin and colleagues (2009).

Statistical analysis

For the growth rate data (Fig. 1), $n = 3$ or $n = 4$, we used a non-parametric, Kruskal–Wallis Test, for analysing variance between groups ($p < 0.05$). This was further verified using a one-way ANOVA ($p < 0.05$) followed by a Scheffe *post hoc* test.

Determining the elemental stoichiometric ratios ($n = 12$–13 per treatment) differences of the five treatments was done by verifying normal distribution using a Kolmogorov-Smirnoff and by using one-way ANOVA ($p < 0.001$). The ANOVA was followed by a Scheffe *post hoc* test that yielded $p < 0.001$ for C : N averages, $p < 0.05$ for C : P averages. For all Scheffe *post hoc* tests, different letters represent significant difference.

Acknowledgements

This work is in partial fulfillment of the requirements for a PhD thesis for O. Levitan at Bar Ilan University, and was conducted as part of the BMBF-MOST grant 1950 to I.B.F. and J.L.R. We wish to thank Ms Diana Hümmer (IFM-GEOMAR) and Ms. Dina Spungin (BIU) for technical help. Also, we thank Dr Ondrej Prasil (Institute. Microbiology, Trebon, Czech Republic) for analysing our C : N samples. Statistical analysis

was performed with the advice of Dr. Rachel S. Levy-Drummer. O. Levitan was supported by a Reiger Fellowship for Environmental Studies and by the Eshkol scholarship from the Israeli ministry of Science, Culture and Sports. C.M. Brown was supported by NSERC.

References

Badger, M.R., and Price, G.D. (2003) CO_2 concentrating mechanisms in cyanobacteria: molecular components, their diversity and evolution. *J Exp Bot* **54:** 609–622.

Badger, M.R., Price, G.D., Long, B.M., and Woodger, F.J. (2006) The environmental plasticity and ecological genomics of the cyanobacterial CO_2 concentrating mechanism. *J Exp Bot* **57:** 249–265.

Berman-Frank, I., Lundgren, P., Chen, Y.B., Kupper, H., Kolber, Z., Bergman, B., and Falkowski, P. (2001a) Segregation of nitrogen fixation and oxygenic photosynthesis in the marine cyanobacterium *Trichodesmium*. *Science* **294:** 1534–1537.

Berman-Frank, I., Cullen, J.T., Shaked, Y., Sherrell, R.M., and Falkowski, P.G. (2001b) Iron availability, cellular iron quotas, and nitrogen fixation in *Trichodesmium*. *Limnol Oceanogr* **46:** 1249–1260.

Berman-Frank, I., Quigg, A., Finkel, Z.V., Irwin, A.J., and Haramaty, L. (2007) Nitrogen fixation strategies and Fe requirements in cyanobacteria. *Limnol Oceanogr* **52:** 2260–2269.

Bonnet, S., Guieu, C., Bruyant, F., Prasil, O., Van Wambeke, F., Raimbault, P., *et al.* (2008) Nutrient limitation of primary productivity in the Southeast Pacific (BIOSOPE cruise). *Biogeosciences* **5:** 215–225.

Bonnet, S., Biegala, I.C., Dutrieux, P., Slemons, L.O., and Capone, D.G. (2009) Nitrogen fixation in the western equatorial Pacific: rates, diazotrophic cyanobacterial size class distribution, and biogeochemical significance. *Global Biogeochem Cycles* **23:** 1–13.

Breitbarth, E., Oschlies, A., and LaRoche, J. (2007) Physiological constraints on the global distribution of *Trichodesmium* – effect of temperature on diazotrophy. *Biogeosciences* **4:** 53–61.

Brown, C.M., MacKinnon, J.D., Cockshutt, A.M., Villareal, T.A., and Campbell, D.A. (2008) Flux capacities and acclimation costs in *Trichodesmium* from the Gulf of Mexico. *Mar Biol* **154:** 413–422.

Bustin, S.A., Benes, V., Garson, J.A., Hellemans, J., Huggett, J., Kubista, M., *et al.* (2009) The MIQE guidelines: minimum information for publication of quantitative real-time PCR experiments. *Clin Chem* **55:** 611–622.

Capone, D.G. (1993) Determination of Nitrogenase activity in aquatic samples using the acetylene reduction procedure. In *Handbook of Methods in Aquatic Microbial Ecology*. Kemp, P.F., Sherr, B., Sherr, E., and Cole, J. (eds). New York, NY, USA: Lewis Publishers, pp. 621–631.

Capone, D.G., and Montoya, J.P. (2001) Nitrogen fixation and denitrification. *Methods Microbiol* **30:** 501–515.

Capone, D.G., and Subramaniam, A. (2005) Seeing microbes from space – remote sensing is now a critical resource for tracking marine microbial ecosystem dynamics and their impact on global biogeochemical cycles. *ASM News* **71:** 179–196.

Capone, D.G., Oneil, J.M., Zehr, J., and Carpenter, E.J. (1990) Basis for diel variation in nitrogenase activity in the marine planktonic cyanobacterium *Trichodesmium thiebautii*. *Appl Environ Microbiol* **56:** 3532–3536.

Capone, D.G., Zehr, J.P., Paerl, H.W., Bergman, B., and Carpenter, E.J. (1997) *Trichodesmium*, a globally significant marine cyanobacterium. *Science* **276:** 1221–1229.

Carpenter, E.J., and Capone, D.G. (2008) Nitrogen fixation in the marine environment. In *Nitrogen in the Marine Environment*, 2nd edn. Capone, D., Bronk, D., Mulholland, M., and Carpenter, E. (eds). San Diego, CA, USA: Academic Press, pp. 141–198.

Carpenter, E.J., Bergman, B., Dawson, R., Siddiqui, P.J., Soderback, E., and Capone, D.G. (1992) Glutamine synthetase and nitrogen cycling in colonies of the marine diazotrophic cyanobacteria *Trichodesmium* spp. *Appl Environ Microbiol* **58:** 3122–3129.

Chen, Y.B., Zehr, J.P., and Mellon, M. (1996) Growth and nitrogen fixation of the diazotrophic filamentous nonheterocystous cyanobacterium *Trichodesmium* sp IMS 101 in defined media: Evidence for a circadian rhythm. *J Phycol* **32:** 916–923.

Chen, Y.B., Dominic, B., Mellon, M.T., and Zehr, J.P. (1998) Circadian rhythm of nitrogenase gene expression in the diazotrophic filamentous nonheterocystous Cyanobacterium *Trichodesmium* sp strain IMS101. *J Bacteriol* **180:** 3598–3605.

Chen, Y.B., Dominic, B., Zani, S., Mellon, M.T., and Zehr, J.P. (1999) Expression of photosynthesis genes in relation to nitrogen fixation in the diazotrophic filamentous nonheterocystous cyanobacterium *Trichodesmium* sp IMS 101. *Plant Mol Biol* **41:** 89–104.

Church, M.J., Bjorkman, K.M., Karl, D.M., Saito, M.A., and Zehr, J.P. (2008) Regional distributions of nitrogen-fixing bacteria in the Pacific Ocean. *Limnol Oceanogr* **53:** 63–77.

Davis, C.S., and McGillicuddy, D.J. (2006) Transatlantic abundance of the N_2 fixing colonial cyanobacterium *Trichodesmium*. *Science* **312:** 1517–1520.

Dominic, B., Chen, Y.B., and Zehr, J.P. (1998) Cloning and transcriptional analysis of the *nifUHDK* genes of *Trichodesmium* sp. IMS101 reveals stable *nifD, nifDK* and *nifK* transcripts. *Microbiology-UK* **144:** 3359–3368.

El-Shehawy, R., Lugomela, C., Ernst, A., and Bergman, B. (2003) Diurnal expression of hetR and diazocyte development in the filamentous non-heterocystous cyanobacterium *Trichodesmium erythraeum*. *Microbiology-Sgm* **149:** 1139–1146.

Flores, E., and Herrero, A. (1994) Assimilatory nitrogen metabolism and its regulation. In *The Molecular Biology of Cyanobacteria*. Bryant, D.A. (ed.). Dordrecht, the Netherlands: Kluwer Scientific Publications, pp. 487–517.

Hageman, R.V., and Burris, R.H. (1978) Kinetic studies on electron-transfer and interaction between nitrogenase components from *Azotobacter vinelandii*. *Biochemistry* **17:** 4117–4124.

Holl, C.M., and Montoya, J.P. (2008) Diazotrophic growth of the marine cyanobacterium *Trichodesmium* IMS101 in continuous culture: effects of growth rate on N_2 fixation rate, biomass, and C : N : P stoichiometry. *J Phycol* **44:** 929–937.

Hutchins, D.A., Fu, F.-X., Zhang, Y., Warner, M.E., Portune, K., Bernhardt, P.W., and Mulholland, M.R. (2007) CO_2 control of *Trichodesmium* N_2 fixation, photosynthesis, growth rates, and elemental ratios: implications for past, present, and future ocean biogeochemistry. *Limnol Oceanogr* **52:** 1293–1304.

Kramer, J.G., Wyman, M., Zehr, J.P., and Capone, D.G. (1996) Diel variability in transcription of the structural gene for glutamine synthetase (*glnA*) in natural populations of the marine diazotrophic cyanobacterium *Trichodesmium thiebautii*. *FEMS Microbiol Ecol* **21:** 187–196.

Kranz, S., Sültemeyer, D., Richter, K.-U., and Rost, B. (2009) Carbon acquisition by *Trichodesmium*: the effect of pCO_2 and diurnal changes. *Limnol Oceanogr* **54:** 548–559.

Krauk, J.M., Villareal, T.A., Sohm, J.A., Montoya, J.P., and Capone, D.G. (2006) Plasticity of N : P ratios in laboratory and field populations of *Trichodesmium* spp. *Aquat Microb Ecol* **42:** 243–253.

Küpper, H., Ferimazova, N., Setlik, I., and Berman-Frank, I. (2004) Traffic lights in *Trichodesmium*. Regulation of photosynthesis for nitrogen fixation studied by chlorophyll fluorescence kinetic microscopy. *Plant Physiol (Rockville)* **135:** 2120–2133.

Küpper, H., Setlik, I., Seibert, S., Prasil, O., Setlikova, E., Strittmatter, M., *et al.* (2008) Iron limitation in the marine cyanobacterium *Trichodesmium* reveals new insights into regulation of photosynthesis and nitrogen fixation. *New Phytol* **179:** 784–798.

Lanzilotta, W.N., and Seefeldt, L.C. (1996) Electron transfer from the nitrogenase iron protein to the [8Fe-(7/8)S] clusters of the molybdenum-iron protein. *Biochemistry* **35:** 16770–16776.

LaRoche, J., and Breitbarth, E. (2005) Importance of the diazotrophs as a source of new nitrogen in the ocean. *J Sea Res* **53:** 67–91.

Levitan, O., Rosenberg, G., Setlik, I., Setlikova, E., Grigel, J., Klepetar, J., *et al.* (2007) Elevated CO_2 enhances nitrogen fixation and growth in the marine cyanobacterium *Trichodesmium*. *Global Change Biol* **13:** 531–538.

Lin, S.J., Henze, S., Lundgren, P., Bergman, B., and Carpenter, E.J. (1998) Whole-cell immunolocalization of nitrogenase in marine diazotrophic cyanobacteria, *Trichodesmium* spp. *Appl Environ Microbiol* **64:** 3052–3058.

Livak, K., and Schmittgen, T. (2001) Analysis of relative gene expression data using real-time quantitative PCR and the $2^{-\Delta\Delta Ct}$ method. *Methods* **25:** 402–408.

MacIntyre, H.L., and Cullen, J.J. (2005) Using cultures to investigate the physiological ecology of microalgae. In *Algal Culturing Techniques*. Anderson, R.A. (ed.). Burlington, MA, USA: Elsevier Academic Press, pp. 287–326.

Mahaffey, C., Michaels, A.F., and Capone, D.G. (2005) The conundrum of marine N_2 fixation. *Am J Sci* **305:** 546–595.

Milligan, A.J., Berman-Frank, I., Gerchman, Y., Dismukes, G.C., and Falkowski, P.G. (2007) Light-dependent oxygen consumption in nitrogen-fixing cyanobacteria plays a key role in nitrogenase protection. *J Phycol* **43:** 845–852.

Mills, M.M., Ridame, C., Davie, M., La Roche, J., and Geider, R.J. (2004) Iron and phosphorus co-limit nitrogen fixation in the eastern tropical North Atlantic. *Nature* **429:** 292–294.

Mulholland, M.R., and Capone, D.G. (1999) Nitrogen fixation, uptake and metabolism in natural and cultured populations of *Trichodesmium* spp. *Mar Ecol Prog Ser* **188:** 33–49.

Mulholland, M.R., and Capone, D.G. (2000) The nitrogen physiology of the marine N_2 fixing cyanobacteria *Trichodesmium* spp. *Trends Plant Sci* **5:** 148–153.

Mulholland, M.R., Ohki, K., and Capone, D.G. (1999) Nitrogen utilization and metabolism relative to patterns of N_2 fixation in cultures of *Trichodesmium* NIBB1067. *J Phycol* **35:** 977–988.

Ohkawa, H., Sonoda, M., Shibata, M., and Ogawa, T. (2001) Localization of NAD(P)H dehydrogenase in the cyanobacterium *Synechocystis* sp. strain PCC 6803. *J Bacteriol* **183:** 4938–4939.

Postgate, J.R. (1998) *Nitrogen Fixation*. Cambridge, UK: Cambridge University Press.

Price, G.D., and Badger, M.R. (2002) Advances in understanding how aquatic photosynthetic organisms utilize sources of dissolved inorganic carbon for CO_2 fixation. *Funct Plant Biol* **29:** 117–121.

Ramakers, C., Ruijter, J.M., Deprez, R.H.L., and Moorman, A.F.M. (2003) Assumption-free analysis of quantitative real-time PCR data. *Neurosci Lett* **339:** 62–66.

Ramos, B.J., Biswas, H., Schulz, K., LaRoche, J., and Riebesell, U. (2007) Effect of rising atmospheric carbon dioxide on the marine nitrogen fixer *Trichodesmium*. *Global Biogeochem Cycles* **21:** 1–6.

Raven, J.A. (1997) Inorganic carbon acquisition by marine autotrophs. *Adv Bot Res* **27:** 85–209.

Raymond, J., Siefert, J.L., Staples, C.R., and Blankenship, R.E. (2004) The natural history of nitrogen fixation. *Mol Biol Evol* **21:** 541–554.

Reade, J.P.H., Dougherty, L.J., Rogers, L.J., and Gallon, J.R. (1999) Synthesis and proteolytic degradation of nitrogenase in cultures of the unicellular cyanobacterium *Gloeothece* strain ATCC 27152. *Microbiology-UK* **145:** 1749–1758.

Scanlan, D.J., and Wilson, W.H. (1999) Application of molecular techniques to addressing the role of P as key effector in marine ecosystems. *Hydrobiologia* **401:** 149–175.

Tandeau De Marsac, N., and Houmard, J. (1988) Complementary chromatic adaptation: physiological conditions and action spectra. In *Cyanobacteria*. Packer, L., and Glazer, A.N. (eds). San Diego, CA, USA: Academic Press, pp. 318–328.

Tortell, P.D., Rau, G.H., and Morel, M.M.F. (2000) Inorganic carbon acquisition in costal Pacific phytoplankton communities. *Limnol Oceanogr* **45:** 1485–1500.

Vichitphan, K. (2001) *Azotobacter vinelandii* Nitrogenase: Effect of Amino-acid Substitutions at the αGln-191 Residue of the MoFe Protein on Substrate Reduction and CO Inhibition. PhD Thesis. Blacksburg, VA, USA: Virginia Polytechnic Institute and State University.

White, A.E., Spitz, Y.H., Karl, D.M., and Letelier, R.M. (2006) Flexible elemental stoichiometry in *Trichodesmium* spp. and its ecological implications. *Limnol Oceanogr* **51:** 1777–1790.

Zehr, J.P., Ohki, K., and Fujita, Y. (1991) Arrangement of nitrogenase structural genes in an aerobic filamentous nonheterocystous cyanobacterium. *J Bacteriol* **173:** 7055–7058.

Zehr, J.P., Wyman, M., Miller, V., Duguay, L., and Capone, D.G. (1993) Modification of the Fe protein of nitrogenase in Natural populations of *Trichodesmium thiebautii*. *Appl Environ Microbiol* **59:** 669–676.

Zehr, J.P., Harris, D., Dominic, B., and Salerno, J. (1997) Structural analysis of the *Trichodesmium* nitrogenase iron protein: implications for aerobic nitrogen fixation activity. *FEMS Microbiol Lett* **153:** 303–309.

Zhang, J.-Y., Chen, W.-L., and Zhang, C.-C. (2009) *hetR* and *patS*, two genes necessary for heterocyst pattern formation, are widespread in filamentous nonheterocyst-forming cyanobacteria. *Microbiology* **155:** 1418–1426.